Mon. Not. R. Astron. Soc. **000**, 000–000 (0000) Printed 27 February 2015 (MN LATEX style file v2.2)

Warm exo-Zodi from cool exo-Kuiper belts: the significance of P-R drag and the inference of intervening planets

Grant M. Kennedy⋆[1], Anjali Piette[2]
[1] *Institute of Astronomy, University of Cambridge, Madingley Road, Cambridge CB3 0HA, UK*
[2] *Pembroke College, Trumpington Street, Cambridge CB2 1RF, UK*

27 February 2015

ABSTRACT
Poynting-Robertson drag has been considered an ineffective mechanism for delivering dust to regions interior to the cool Kuiper belt analogues seen around other Sun-like stars. This conclusion is however based on the very large contrast in dust optical depth between the parent belt and the interior regions that results from the dominance of collisions over drag in systems with detectable cool belts. Here, we show that the levels of habitable zone dust arising from detectable Kuiper belt analogues can be tens to a few hundreds of times greater than the optical depth in the Solar Zodiacal cloud. Dust enhancements of more than a few tens of 'zodi' are expected to hinder future Earth-imaging missions, but relatively few undetectable Kuiper belts result in such levels, particularly around stars older than a few Gyr. Thus, current mid to far-IR photometric surveys have already identified most of the 20-25% of nearby stars where P-R drag from outer belts could seriously impact Earth-imaging. The LBTI should easily detect such warm dust around many nearby stars with outer belts, and will provide insight into currently unclear details of the competition between P-R drag and collisions. Given sufficient confidence in future models, the inevitability of P-R drag means that the non-detection of warm dust where detectable levels were expected could be used to infer additional dust removal process, the most likely being the presence of intervening planets.

Key words: circumstellar matter — zodiacal dust — planets and satellites: detection — radiation: dynamics

1 INTRODUCTION

As the regions deemed most likely to harbour alien life, the habitable zones of other stars are becoming of increasing interest. Major efforts to find potentially habitable planets are underway (e.g. *Kepler*, PLATO, Borucki et al. 2003; Rauer et al. 2014), with the goal of pushing the detection limits towards true Earth-analogues. Coupled to this interest has been parallel work on exo-Zodiacal dust, both as a potentially useful dynamical tracer that reveals unseen planets (e.g. Stark & Kuchner 2008), and as a source of noise and confusion that may hinder the direct detection and characterisation of such planets (Defrère et al. 2010; Roberge et al. 2012; Stark et al. 2014; Brown 2015).

Habitable zone (HZ) dust is indeed seen around other stars (e.g. Song et al. 2005; Fujiwara et al. 2010), though these detections are limited by the photometric methods used to relatively high dust levels that are rare (Kennedy & Wyatt 2013). In general the origin of this exo-Zodiacal ('exo-zodi') dust is unknown. In some cases, particularly for main-sequence stars, the levels are sufficiently extreme that the dust cannot simply originate in massive analogues of our Asteroid belt because collisional decay would have ground the dust levels well below those observed over the stellar lifetime (Wyatt et al. 2007a). Possible solutions are that the dust was created in a recent collision (i.e. is transient, e.g. Song et al. 2005; Meng et al. 2012), or that the dust is being continuously delivered in the form of comets from more distant regions (e.g. Wyatt et al. 2007a; Bonsor et al. 2012).

Curiously, the mechanism responsible for delivering much of the Zodiacal dust from exterior regions to the Earth's vicinity, Poynting-Robertson (P-R) drag, can be ruled out in almost all extra-Solar cases. The reason is that particles spiralling in by P-R drag are also subject to collisional destruction and subsequent radiation-pressure blowout (for stars more luminous than the Sun, see Reidemeister et al. 2011). The fate of dust created in a parent belt of asteroids or comets (i.e. a 'debris disk') therefore depends on the relative importance of P-R drag and collisions. This issue was explored by Wyatt (2005), who used a

⋆ Email: gkennedy@ast.cam.ac.uk

simple model of P-R drag for dust of a single particle size (see also Wyatt et al. 1999). The key points were: i) the denser the parent belt, the greater the contrast in optical depth between the parent belt and the inner regions, ii) the denser the parent belt, the greater the absolute dust level in the inner regions up to some maximum level, and iii) the debris disks that are detected around other stars are generally collision dominated, rather than P-R drag dominated, and hence P-R drag could be considered insignificant. The motivation was to show that the invocation of extra forces (e.g. unseen planets) was not necessary to explain why the regions interior to some cool disks were not filled in. That is, the model was largely considered within the context of the relative levels of dust in the parent belts and in the interior regions.

An aspect of the model that was not explored in detail by Wyatt (2005) was the absolute level of interior dust, in part because this was not the primary motivation, but also because observations at the time were not sensitive enough to detect the dust levels predicted. However, new instruments are pushing the sensitivity limits for warm dust to levels low enough that P-R drag as an origin of habitable zone dust is becoming relevant. While the photometric methods used to discover bright dust are limited to mid-IR disk to star flux ratios greater than about 10% (at 3σ), the Keck Interferometer Nuller (KIN, Serabyn et al. 2012) was able to reach levels closer to 1% (Millan-Gabet et al. 2011; Mennesson et al. 2014), and the Large Binocular Telescope Interferometer (LBTI, Hinz 2009; Defrère et al. 2015) is expected to go below 0.1%.

Specifically, Mennesson et al. (2014) report new results from the KIN, showing that the level of warm dust seen around nearby stars tends to be higher in systems with detections of cool Kuiper belt analogues. The surprising aspect is that in most cases the levels tend to be similar, a few hundred times the Solar System level. The typical explanation for a direct link between warm and cool belts is comet delivery by planet scattering (e.g. Bonsor & Wyatt 2012; Bonsor et al. 2012), but the outcome of this scenario depends sensitively on various parameters such as the planetary system architecture, so is an unlikely explanation. In contrast, the competition between P-R drag and collisions naturally leads to warm dust levels that are relatively insensitive to the properties of the parent belt, and Mennesson et al. (2014) show that their results are consistent with levels expected from the Wyatt (2005) model of P-R drag delivery

Here, we consider the wider implications of these findings, including the results of van Lieshout et al. (2014) who developed a more sophisticated numerical model of the competition between P-R drag and collisions. Their results are easily incorporated into the analytic model of Wyatt (2005), which we use to make general predictions of the warm dust levels in systems with Kuiper belt analogues.

2 MODEL

2.1 Optical depth interior to parent belt

The steady-state P-R drag model of Wyatt (2005) calculates the dust optical depth as a function of radius interior to a source region, a parent belt of planetesimals where dust is created in collisions between larger bodies. It is an analytic solution of the continuity equation, where the number of particles entering a radial region equals that leaving plus that lost to collisions. The main assumptions were that particles have a single size, and that all collisions were destructive and result in permanent loss of the fragments due to stellar radiation pressure. The model does not therefore apply to stars with insufficient luminosity or stellar wind pressure to blow small dust out of the system (see Augereau & Beust 2006; Reidemeister et al. 2011; Lestrade et al. 2012; Schüppler et al. 2014, for discussions of this case).

Particles at some outer radius r_0, representing the parent belt, have a face-on geometric optical depth τ_0, and the only remaining free parameters are the stellar mass and the strength of the P-R drag on the particles. The latter is parameterised by the ratio of the force felt by a particle due to radiation pressure to the gravitational force, $\beta = F_{\rm rad}/F_\star \propto L_\star/M_\star$ (i.e. we assume that the analogous stellar wind drag effect is relatively small). Small particles created on initially circular orbits are blown out of the system on a dynamical timescale when $\beta > 0.5$, so the model assumed $\beta = 0.5$.

A numerical version of this model was developed by van Lieshout et al. (2014), who included a dust size distribution and accounted for the fact that grains of different sizes are affected to differing degrees by both radiation pressure and P-R drag, and also have different collisional lifetimes due to differences in orbital eccentricity, strength and their relative numbers. Compared to the analytic model, the only significant difference was that the dust levels in the regions interior to the parent belt were nearly an order of magnitude lower. The reason is that the smallest bound grains are created on highly eccentric orbits meaning that collisions are more frequent and at higher relative velocities, so a given particle can be destroyed by a smaller (more common) impactor. They found that interior to the parent belt, the size distribution is dominated by grains near the blowout size, which is consistent with the single grain size assumed in the analytic model. They only explored cases in which the parent belt was relatively massive, so it seems likely that this conclusion arises due to the dominance of collisions immediately interior to the parent belt, where larger grains are heavily depleted by the more numerous near-blowout size grains. In the case where collisions are much less important larger grains would be expected to dominate because of their slower P-R drag timescale. Our focus here is to relate observations to detectable parent belts, so the approximation of a single grain size at the blowout limit is reasonable, but more numerical work is needed to see how the results change with the parent belt optical depth.

For relatively dense parent belts a simple way to include the effect of elliptical orbits in the analytic model is to change the collision timescale by a multiplicative factor, k. The solution to the continuity equation for the optical depth, $\tau(r)$, is

$$\tau(r) = \tau_0 / \left[1 + 4\eta_0 \left(1 - \sqrt{r/r_0}\right)\right], \quad (1)$$

$$\eta_0 = 5000\tau_0 \sqrt{(r_0/a_\oplus)(M_\odot/M_\star)}/(\beta k). \quad (2)$$

These equations only differ from those in Wyatt (2005) by the factor k. Given the results of van Lieshout et al. (2014), we can assume that $\beta = 0.5$ because these grains dominate the size distribution. We set $k = 1$ to represent the original Wyatt (2005) model, which is consistent with the KIN results and is referred to as the "low collision rate", or set $k = 1/7$ to match the numerical model of van Lieshout et al. (2014), which we refer to as the "high collision rate". In the absence of the KIN results we would prefer the high collision rate because it was derived

by a model thought to be more realistic. However, an apparently lower collision rate could arise because the numerical model does not include all important physical effects, for example if not all collisions result in destruction and subsequent blowout (e.g. Krijt & Kama 2014). One of our goals is therefore to make predictions for each case so that observations can empirically find which is more realistic.

To convert the dust optical depth given by eq. (1) into an observable flux density, we follow Wyatt (2005) and assume the emission is from grains that behave as black bodies. Though the dust can in some cases be small enough to be hotter than a black body at a given distance from the star, tests using realistic grain properties find that this approximation is reasonable (and if anything an underestimate of the flux) when calculating mid-IR emission; for A-type stars the smallest grains are large enough to behave approximately as blackbodies, and for later type stars the inefficient emission at wavelengths longer than the grain size is offset by their increased temperatures and consequently greater fluxes.

2.2 Observed Kuiper belt analogues

To connect observations of Kuiper belt analogues to the parent belt properties in the model, we must convert them to our model parameters r_0 and τ_0. The radius can be easily derived from the dust temperature of an observed disk assuming blackbody properties, with the caveat that these estimates are typically a factor of a few too low, depending on the spectral type of the star (e.g. Rodriguez & Zuckerman 2012; Booth et al. 2013; Pawellek et al. 2014). In any case, as we show below, an uncertain radius has a relatively small impact on the model predictions. The optical depth can be estimated from the fractional luminosity $f = L_{\rm disk}/L_\star = \sigma/(4\pi r_0^2)$, where σ is the surface area of emitting dust, with the assumption of some fractional disk width via $\sigma = 2\pi r_0 \Delta r \tau_0$. Again, as we show below the habitable zone dust levels are relatively insensitive to the optical depth of the parent belt, so here we assume $\Delta r = 0.5 r_0$, and thus $\tau_0 = 4f$.

For a sample of known Kuiper belt analogues we use stars from the Unbiased Nearby Stars (UNS) sample (Phillips et al. 2010). Most of these have been observed with *Spitzer* and/or *Herschel* (e.g. Rieke et al. 2005; Trilling et al. 2008; Eiroa et al. 2013; Thureau et al. 2014), and here we use disk properties derived from this far-IR photometry to show a representative disk population. The stellar photospheres have been modelled with PHOENIX AMES-Cond models (Brott & Hauschildt 2005) and the excess fluxes with blackbodies to derive the dust temperatures and luminosities, which are the quantities of interest here (e.g. Kennedy et al. 2012b,a; Thureau et al. 2014). These belts have radii of a few au to a few hundred au, and fractional luminosities between 10^{-6} and 10^{-3}.

3 HABITABLE ZONE DUST LEVELS

3.1 An example

Fig. 1 shows radial optical depth profiles for a Sun-like star for both collision rates and several different parent belt parameters. The outer belt parameters are chosen to represent a relatively bright Kuiper belt analogue, and one near the current detection limit. The optical depth of the Solar Zodiacal cloud (i.e. 1 'zodi' unit of dust) is shown from 0.5 to 2 au (Kelsall et al. 1998).

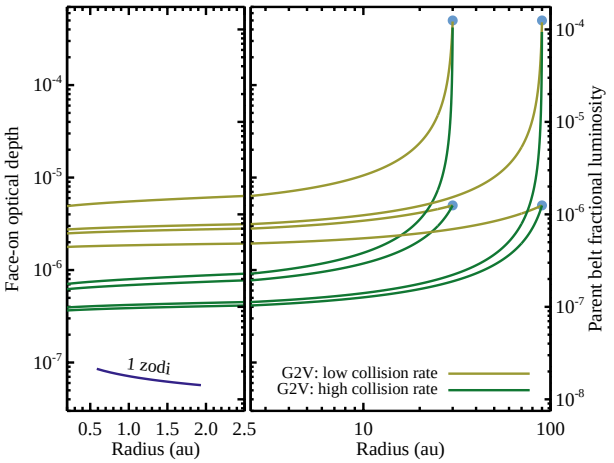

Figure 1. Examples of radial optical depth profiles interior to parent belts around a Sun-like star. The left-hand panel shows a linear radial scale while the right-hand panel is logarithmic. Four different parent belts are shown as dots, with $r_0 = 30$ and 90 au, and $\tau_0 = 5 \times 10^{-6}$ and 5×10^{-4}. The darker lines show the high collision rate ($k = 1/7$) and lighter lines show the low collision rate ($k = 1$). The Solar System's Zodiacal cloud level ('1 zodi') is also shown from 0.5 to 2 au. The dust optical depth in the habitable zone is near-constant, and depends strongly on the collision rate and weakly on the optical depth in the parent belt.

Dust is created in the parent belt with optical depth τ_0, and then moves towards the star due to P-R drag, being depleted by collisions on the way. The collision rate depends on the optical depth, so eventually P-R drag dominates. The P-R drag time is $\propto 1/r$ so the optical depth approaches a constant level with radius. Thus, the optical depth interior to very tenuous parent belts (where collisions are unimportant) is also constant.

For denser parent belts the interior levels become insensitive to the parameters. More dust drifts inwards from denser belts, but this extra dust is also collisionally depleted more rapidly. For fixed stellar parameters and parent belt radius, the interior optical depth reaches a maximum optical depth near the star as τ_0 is increased (i.e. $n_0 \gg 1$ and $\tau(r)$ is independent of τ_0, Wyatt 2005). This insensitivity to parent belt properties is an important aspect of the model that is not expected in other scenarios, where stochastic behaviour and/or strong dependence on system architecture are expected to lead to a wide variety of habitable zone dust levels (e.g. Kennedy & Wyatt 2013; Bonsor & Wyatt 2012). However, the inner dust levels depend strongly on the collision rate assumed (i.e. k). For the examples in Fig. 1 the high collision rate predicts dust levels that are approximately 10 times the Solar Zodiacal level, and the low collision rate levels about 50 times larger. In either case, in the absence of effects that remove the inward moving dust, the regions interior to Kuiper belt analogues seen around other stars (with $f > 10^{-6}$) will have dust levels that are significantly higher than the Solar Zodiacal level.

In the outer Solar System the dust level interior to the Edgeworth-Kuiper belt, with $\tau \sim 10^{-7}$ (Vitense et al. 2012), is thought to be constant in to about 10 au, where most of the particles are ejected by Saturn and Jupiter (estimates of the fraction reaching Earth's vicinity depend on grain size, and vary

from 0-20%, Liou et al. 1996; Kuchner & Stark 2010). The optical depth of the Asteroid belt is similar (Dermott et al. 2002), but most of the dust that spirals in towards the Earth is not lost. Given the uncertainties in their inferred optical depths and models, both have been considered a source for our Zodiacal cloud (Liou et al. 1996; Grogan et al. 2001). In reality, both contribute at some level, and material from Jupiter-family comets serves as a third and equally important source (i.e. dynamical rather then P-R drag delivery from the Kuiper belt, Whipple et al. 1967; Nesvorný et al. 2010). Thus, external observations of the Solar System's dust complement (that might not detect the gap between $\sim$3-5 au), might reasonably conclude that the Zodiacal dust originates in the Kuiper belt and is delivered by P-R drag. However, our knowledge of the actual architecture shows that planets can strongly influence the habitable zone dust level, both depleting it relative to simple expectations by removing dust as it spirals in, and enhancing it by allowing other delivery mechanisms.

3.2 Model predictions

Fig. 2 shows predicted dust levels in the habitable zone for an A-type and a Sun-like star. We use the concept of the "Earth-equivalent insolation distance" (EEID) as a simple definition of the habitable zone location, which is simply equal to $\sqrt{L_\star/L_\odot}$ in units of au (i.e. 1 au for the Sun, Roberge et al. 2012). In each panel contours show the dust level at the EEID, relative to the Solar System optical depth at 1 au of 7.12×10^{-8} (Kelsall et al. 1998), for a range of parent belt optical depths and radii. That is, at the EEID (but not necessarily elsewhere) these contours are the same as the "zodi" units defined in Kennedy et al. (2015) for the purposes of LBTI modelling. Sub-panels for both the high and low collision rate models are shown. The symbols mark known Kuiper belt analogues seen around nearby stars from the sample of (Phillips et al. 2010), including a 'tail' that reflects the approximate systematic uncertainty in the dust radial location. Vertical uncertainties are relatively small (roughly a factor $\pm$2) as any model that fits the disk photometry will have a similar integrated luminosity. A representative detection limit for the parent belts around nearby stars with mid and far-IR photometry (24 and 100 μm) is shown (computed as in Wyatt 2008), where detections are possible above the dashed line, and differs for A and G-type stars because their luminosities are different. At low parent belt densities the dust level contours are roughly constant with radius because P-R drag dominates. At high densities collisions dominate and the habitable zone dust level depends only on the radial proximity of the parent belt to the habitable zone.

Thus, P-R drag of dust from known Kuiper belt analogues can result in significant HZ dust levels relative to the Solar System level, regardless of the assumed collision rate. The results clearly depend on the adopted collision rate; the low collision rate implied by the KIN results suggests that the HZ dust level is typically 50-500 times the Solar Zodiacal level for detectable parent belts around Sun-like and A-type stars. The higher collision rate results in typical levels closer to 10-100 times the Solar Zodiacal level.

The nature of the photometric detection limits means that there is a region of the parameter space in all cases where HZ dust levels in excess of a few tens of times the Solar System level can arise from belts that cannot be detected by photometry. These parent belts tend to be close to the habitable zone however, and therefore decay by collisions faster than belts that are farther out, mostly due to higher relative velocities. The approximate maximum optical depth of a parent belt in collisional equilibrium is shown in each panel, for average stellar ages of 500 Myr and 5 Gyr, using planetesimal properties that fit their observed brightness evolution (Wyatt et al. 2007b; Kains et al. 2011). The vertical position of these lines varies as $1/t_{\rm age}$, and for a given age few belts are seen or expected above such lines (e.g. Wyatt et al. 2007a). Thus, the space where belts are allowed by collisional evolution but are not detectable and result in significant HZ dust levels is relatively small, and decreases in size as the age of the star increases.

4 DISCUSSION

Poynting-Robertson drag is one of many ways to produce habitable zone dust, the main alternatives being material produced locally in collisions or dynamical comet delivery by planet scattering. Thus, where a Kuiper belt analogue is known the exo-zodi levels discussed above are maximum P-R drag induced dust levels that can be compared with observations to draw conclusions about the dust origin. That is, dust levels significantly greater than predicted require a different origin.

For example, the most extreme system known to harbour warm and cool dust populations is the F2V star η Corvi (e.g. Wyatt et al. 2005; Smith et al. 2009; Defrère et al. 2015), where the location and optical depth of the warm belt is roughly 1 au and 10^{-3}, and 150 au and 10^{-4} for the cool belt. Fig. 1 shows that the HZ optical depth expected from any parent belt from P-R drag is lower than 10^{-5}, and therefore that the warm dust is not delivered from the outer belt by P-R drag. Indeed, the only systems where such bright warm dust may originate in cool belts are those with low stellar luminosities, where collisions during inspiral do not result in removal, and thus the interior optical depth remains approximately the same as in the parent belt (e.g. ϵ Eri, Reidemeister et al. 2011). In general therefore, detections of warm dust well above the predictions of the P-R drag models around Solar and earlier-type stars require a different origin. In the case of η Crv the favoured scenario is that comets are being scattered inward from the cool belt by unseen planets (e.g. Wyatt et al. 2007a; Lisse et al. 2012).

4.1 Habitable zone dust levels

It seems probable that all stars host cool outer debris disks, with only the brightest 20-25% being detectable with current methods (e.g. Trilling et al. 2008; Su et al. 2006; Eiroa et al. 2013; Sierchio et al. 2014; Thureau et al. 2014). Indeed, this was the assumption made in various population models that reasonably reproduce the statistics of such disks (e.g. Wyatt et al. 2007b; Kains et al. 2011; Gáspár et al. 2013). Given the inevitability of P-R drag, this population of cool outer belts implies the existence of a corresponding population of warm dust around all stars. Combined with the results in Fig. 2, the 20-25% of stars with detected cool belts can therefore be used to make some useful statements about HZ dust levels.

For A-type stars, Fig. 2 shows that detectable cool belts result in HZ dust levels at least 20-100 times greater than in the Solar System (i.e. most known outer belts are above these contours). Thus, among the remaining 75-80% of stars the HZ dust levels due to P-R drag are below these levels. For G-type

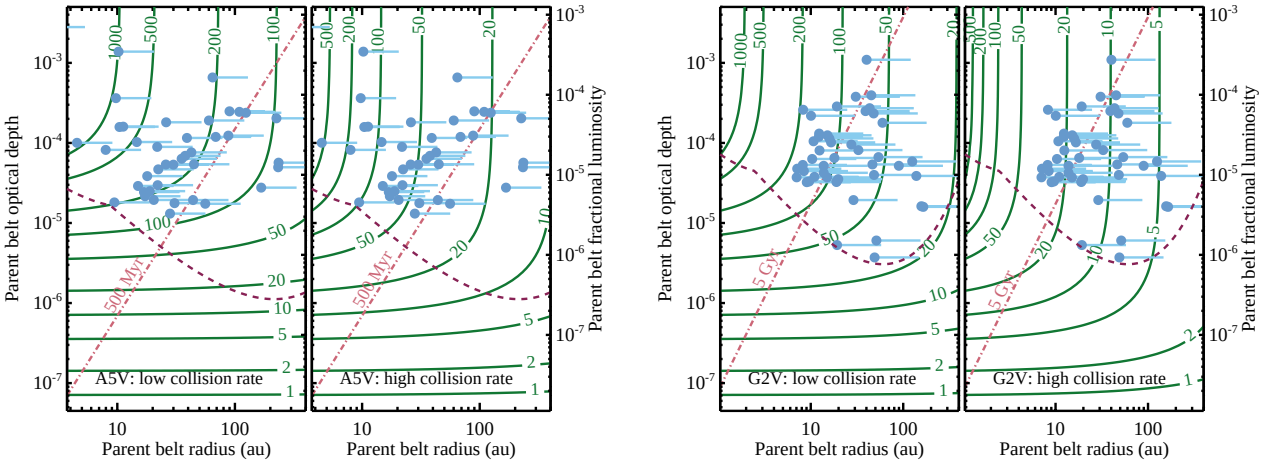

Figure 2. Dust levels at the EEID for an A-type (3.7 au) and a Sun-like (1 au) star for a range of r_0 and τ_0. Contours show the optical depth relative to the Solar System level at 1 au of 7.12×10^{-8}. Dots mark known Kuiper belt analogues around nearby stars and connected lines show the probable increase in size due to non-blackbody emission from small dust. An approximate photometric detection limit is shown by the dashed line. Dot dashed lines show the maximum fractional luminosity as a function of radius for stellar ages of 500 Myr and 5 Gyr (as labelled). For each panel, the left sub-panel shows results for the low collision rate ($k = 1$), and the right sub-panel shows results for the high collision rate ($k = 1/7$). The left end of the radial scale stops at the EEID in each case.

stars the predicted HZ dust levels are lower, and the 75-80% or so of Sun-like stars with no known outer belts have HZ dust below 10-50 times the Solar System level.

Various studies have estimated the impact of HZ dust on future missions that will attempt to detect and characterise Earth-like planets around other stars. The two most recent studies seem to reach a consensus that, with the appropriate survey strategy and under the assumption of smooth exo-zodi, this impact is a relatively weak function of dust brightness, and that for levels below a few tens of times the Solar System level a mission will not be seriously hindered (Stark et al. 2014; Brown 2015). The possible impact of non-axisymmetric structure is less certain however, since inhomogeneities in exo-Zodi surface brightness may themselves be mistaken for planets (e.g. Lay 2004; Defrère et al. 2010). Such structures may of course also be signposts of the dynamical influence of unseen planets (e.g. Stark & Kuchner 2008). Whether such structure presents a major barrier depends both on the typical level of non-axisymmetry and the specifics of the Earth-imaging mission, but could result in a tolerable exo-Zodi level closer to ten times the Solar System level.

Based on our HZ dust predictions, Earth-imaging efforts for Sun-like stars are unlikely to be seriously affected by dust coming in from undetected outer belts, but most of the 20-25% of systems with detected outer belts would be considered unsuitable targets for this reason. For A-type stars such a statement is less certain, as it is possible that 10-30 au belts just below the level of detectability (whose frequency is unknown), will contribute to HZ dust levels. Collisional depletion of the parent belts over time means that this issue can be mitigated to some degree by avoiding young stars. It is unlikely that such belts make up a large fraction of the population however, so the fraction of unsuitable systems is probably not significantly greater than 25%.

Thus, while a non-negligible fraction of stars are expected to be poorly suited to Earth-imaging/characterisation due to P-R drag from outer belts, the detection limits of extant far-IR surveys means that among stars within a few tens of parsec most of these systems are already known. As noted above however, P-R drag is by no means the only origin of habitable zone dust. Thus, in the absence of other effects (see next section) the levels predicted by detections of cool outer belts represent a lower limit on dust in a given system.

4.2 Inference of unseen planets

The inward transport of dust from a known parent belt by P-R drag is inevitable, so additional processes must also be invoked if HZ dust levels could be shown to be significantly lower than expected. That is, something may be needed to remove the dust somewhere between the parent belt and where detection was attempted. By analogy with the Solar System, the most obvious reason is of course accretion or ejection of that dust by intervening planets (Liou et al. 1996; Liou & Zook 1999; Wyatt et al. 1999; Vitense et al. 2012). Whether the dust is accreted or ejected will to first order depend on the ratio of the escape velocity from the planet to the local escape velocity from the star. Thus, a further implication is that close-in planets (e.g. those that transit their stars) are also those most likely to accrete dust, rather than eject it, perhaps with observable effects. The limits set by the KIN were unfortunately not stringent enough to require the explanation of dust removal by other processes for any systems, their Fig. 10 shows that the non-detections are close to or above the levels predicted by the low collision rate model.

Perhaps the most promising system where such a test could be made is around the "retired" A-type star κ CrB. Though the spectral type is K0, the star is a sub-giant and for our purposes can be treated as an A-type star because stellar luminosity and mass are the important model parameters here. This system has a bright outer dust belt that extends from 20-40 au out to 165-220 au depending on the disk model (Bonsor et al. 2013), and at least two companions. One at 2.7 au has been well characterised by radial velocity (Johnson et al. 2008), and another is inferred

to exist at greater distance due to the existence of a residual acceleration in the radial velocity data (Bonsor et al. 2013). With only a constant acceleration seen over 8 years, the outer companion lies beyond about 7 au, and therefore beyond the EEID of 3.5 au. This companion is inferred to be more massive than Jupiter, and resides at a radial distance where the escape velocity from the star is lower, and can therefore easily eject particles that interact with it. Thus, if this companion lies interior to the outer dust belt it will eject much of the dust that would otherwise reach the habitable zone. Given confidence in the P-R drag model, a sufficiently constraining non-detection of warm dust around κ CrB could therefore be used as further evidence of the second companion's existence.

In the Solar System, the Asteroid belt and Jupiter family comets provide alternative habitable zone dust sources, and it seems largely a coincidence that the Zodiacal cloud has approximately the level expected for P-R drag from Kuiper belt dust. As noted in section 3.1, an external observer with similar but moderately more sensitive instruments than ours might conclude that the dust in the inner Solar System is consistent with that expected from P-R drag from the Kuiper belt, and therefore that invoking unseen planets is not necessary. Thus, while additional processes and dust source regions may cause existing planets to be missed, they would not cause non-existent planets to be inferred.

4.3 Detectability with LBTI

An uncertainty in the above predictions for HZ dust levels is which of our two models is more correct. That is, a significant step towards improving the model would be an empirical calibration of the parameter k across a range of stellar spectral types and parent belt properties. We now show that these models will be strongly tested by the LBTI, and hence aid further model development. The LBTI will survey a sample of $\sim$50 nearby stars, with a wide variety of spectral types, to look for habitable zone dust (Weinberger et al. 2015). The sample includes stars known to host cool outer dust belts; a few of these are Sun-like stars but most are earlier A-types.

Briefly, the LBTI is a nulling interferometer that operates in the mid-IR (11 μm), so interferes the light collected by each of the two LBT mirrors to attenuate the starlight. Off-axis mid-IR emission at an angular scale of greater than $\sim$40 mas, for example from warm dust, is transmitted. The attenuation of the starlight avoids the problem of disentangling the dust emission from the stellar emission, which is the limiting factor for discovery of habitable zone dust using purely photometric methods (i.e. sets the dashed lines in Fig. 2). In practice, LBTI observations involve various calibration steps, and for a description of these we refer the reader to Defrère et al. (2015). The key point is that an LBTI measurement, known as the "calibrated null depth" or "null excess", is the ratio of the disk flux that is transmitted though the LBTI fringe pattern to the star+disk flux. Thus, because the disk is almost always much fainter than the star, the null excess can be thought of as analogous to the disk to star flux ratio, but with the disk flux attenuated by the sky projection of the LBTI transmission pattern (Millan-Gabet et al. 2011; Defrère et al. 2015). We use the model outlined by Kennedy et al. (2015), and assume face-on disks to convert our model dust levels to null excesses.

Null excesses are shown as contours in Fig. 3 again for a range of parent belt properties, for both Sun-like and A-type stars and the low and high collision rates. Again, known outer belts around nearby stars and photometric sensitivity limits are also included. The projected LBTI 3σ null excess sensitivity is 3×10^{-4}, so these contours, and a higher level of 10^{-3}, are shown. Because the null excess depends on the angular scale of the disk, the contours show pairs at two different distances (10 and 30 pc). The null excesses always increase with optical depth, so for each distance the contours show the minimum parent belt optical depth for warm dust to be detectable at that level.

Looking first at the low collision rate model (left panels), all of the known parent belts lie in regions where the warm dust is detectable by the LBTI. In addition, for A-stars there is a large swath of parameter space for LBTI detection of warm dust from parent belts that are otherwise undetectable by photometry. A similar region exists for Sun-like stars, but covers less parent belt parameter space. For this model warm dust is therefore predicted to be detectable with LBTI, easily in most cases, for all systems with known Kuiper belt analogues. Thus, if the KIN results of a direct connection between warm and cool dust is the result of P-R drag and the low collision rate model applies across AFG spectral types, the LBTI will strongly confirm this result.

In cases where no parent belt has been seen, warm dust originating in such a belt could still be detected. The origin of this low level HZ dust will be ambiguous; mere detection will be sufficiently difficult that further constraints on the radial extent, which could provide clues to the origin, will be poor (Kennedy et al. 2015; Defrère et al. 2015).

For the high collision rate the results are very similar for A-type stars; nearly all systems with known parent belts should result in LBTI detections. Detections of dust from undetected parent belts also remains possible. For Sun-like stars however, only systems with parent belts with radii $\lesssim$15 au should result in LBTI detections.

5 SUMMARY AND CONCLUSIONS

The development of new instruments means that P-R drag can no longer be considered an insignificant effect for transporting dust to regions interior to the Kuiper belt analogues seen around other stars. While the point that the contrast between a parent belt and the inner regions is high remains, the absolute dust levels interior to known parent belts can be hundreds of times higher than seen in the Solar Zodiacal cloud. We have explored these levels using two flavours of an analytic P-R drag model, connecting the properties of known Kuiper belt analogues to expected habitable zone dust levels.

Habitable zone dust levels greater than a few tens of times the Solar System level will be detrimental to future missions to discover and characterise Earth-like planets around other stars. Currently detectable Kuiper belt analogues are predicted to result in HZ dust levels similar to this limit. Thus, mid and far-IR debris disk surveys have already identified most of the 20-25% of stars where P-R drag from outer belts could seriously impact Earth-imaging. The existence of other processes that generate/deliver HZ dust of course means that the 20-25% is a lower limit.

A caveat to such predictions is that intervening planets may prevent this dust from reaching the habitable zone, instead being

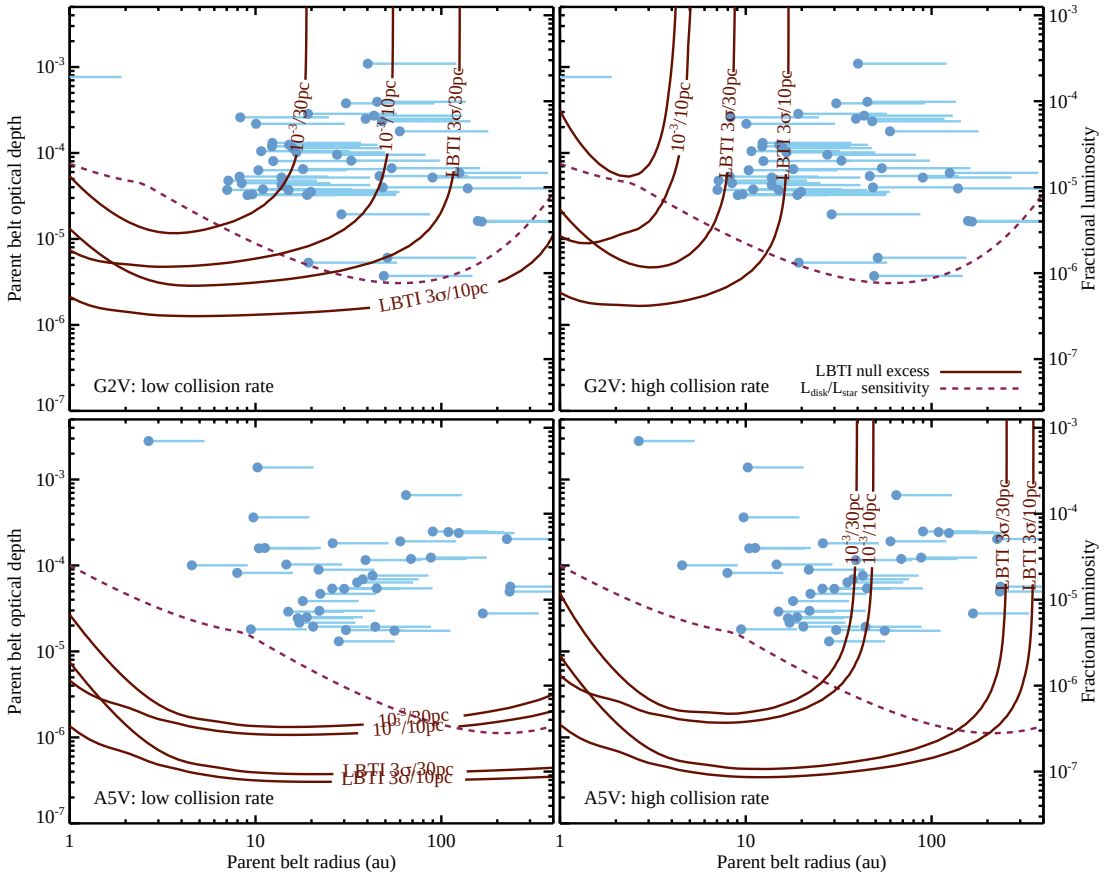

Figure 3. LBTI null excesses for a range of parent belt parameters, for two different sensitivities (3×10^{-4} and 10^{-3}), and two stellar distances (10 and 30pc, contours as labelled). The top row shows models for a Sun-like star, and the bottom row shows models for an A-type star. Left panels show models for the low collision rate, and right panels show models for the high collision rate. Dots mark known Kuiper belt analogues around nearby stars and connected lines show the probable increase in size due to non-blackbody emission from small dust. Dashed lines show approximate detection limits for parent belts around nearby stars. The null excesses always increase with parent belt optical depth, so for each distance the contours show the minimum optical depth for warm dust to be detectable at that level.

ejected or accreted by intervening planets. Thus, in systems with known outer belts the non-detection of such warm dust could, given sufficient confidence in the models, be used to infer the existence of unseen planets. Currently the models are uncertain however, so the goal of future work should therefore be first to empirically calibrate the P-R drag models (e.g. with LBTI observations) to aid model development, and then to interpret the observations within the framework of such a model.

ACKNOWLEDGMENTS

We thank Rik van Lieshout and Mark Wyatt for useful discussions, Bertrand Mennesson for sharing the KIN results ahead of publication, the reviewer for thoughtful and constructive comments, and the LBTI Science and Instrument teams for providing some of the motivation for this work. GMK is supported by the European Union through ERC grant number 279973, and AP gratefully acknowledges support from an Undergraduate Research Bursary from the Royal Astronomical Society.

REFERENCES

Augereau, J.-C. & Beust, H. 2006, A&A, 455, 987
Bonsor, A., Augereau, J.-C., & Thébault, P. 2012, A&A, 548, A104
Bonsor, A., Kennedy, G. M., Crepp, J. R., Johnson, J. A., Wyatt, M. C., Sibthorpe, B., & Su, K. Y. L. 2013, MNRAS, 431, 3025
Bonsor, A. & Wyatt, M. C. 2012, MNRAS, 420, 2990
Booth, M. et al. 2013, MNRAS, 428, 1263
Borucki, W. J., Koch, D. G., Lissauer, J. J., Basri, G. B., Caldwell, J. F., Cochran, W. D., Dunham, E. W., Geary, J. C., Latham, D. W., Gilliland, R. L., Caldwell, D. A., Jenkins, J. M., & Kondo, Y. 2003, in Society of Photo-Optical Instrumentation Engineers (SPIE) Conference Series, Vol. 4854, Society of Photo-Optical Instrumentation Engineers (SPIE) Conference Series, ed. J. C. Blades & O. H. W. Siegmund, 129–140
Brott, I. & Hauschildt, P. H. 2005, in ESA Special Publication, Vol. 576, The Three-Dimensional Universe with Gaia, ed. C. Turon, K. S. O'Flaherty, & M. A. C. Perryman, 565
Brown, R. A. 2015, ApJ, 799, 87
Defrère, D., Absil, O., den Hartog, R., Hanot, C., & Stark, C. 2010, A&A, 509, A9

Defrère, D., Hinz, P. M., Skemer, A. J., Kennedy, G. M., Bailey, V. P., Hoffmann, W. F., Mennesson, B., Millan-Gabet, R., Danchi, W. C., Absil, O., Arbo, P., Beichman, C., Brusa, G., Bryden, G., Downey, E. C., Durney, O., Esposito, S., Gaspar, A., Grenz, P., Haniff, C., Hill, J. M., Lebreton, J., Leisenring, J. M., Males, J. R., Marion, L., McMahon, T. J., Montoya, M., Morzinski, K. M., Pinna, E., Puglisi, A., Rieke, G., Roberge, A., Serabyn, E., Sosa, R., Stapeldfeldt, K., Su, K., Vaitheeswaran, V., Vaz, A., Weinberger, A. J., & Wyatt, M. C. 2015, ApJ, 799, 42
Dermott, S. F., Durda, D. D., Grogan, K., & Kehoe, T. J. J. 2002, Asteroids III, 423
Eiroa, C. et al. 2013, A&A, 555, A11
Fujiwara, H., Onaka, T., Ishihara, D., Yamashita, T., Fukagawa, M., Nakagawa, T., Kataza, H., Ootsubo, T., & Murakami, H. 2010, ApJ, 714, L152
Gáspár, A., Rieke, G. H., & Balog, Z. 2013, ApJ, 768, 25
Grogan, K., Dermott, S. F., & Durda, D. D. 2001, Icarus, 152, 251
Hinz, P. M. 2009, in American Institute of Physics Conference Series, Vol. 1158, American Institute of Physics Conference Series, ed. T. Usuda, M. Tamura, & M. Ishii, 313–317
Johnson, J. A., Marcy, G. W., Fischer, D. A., Wright, J. T., Reffert, S., Kregenow, J. M., Williams, P. K. G., & Peek, K. M. G. 2008, ApJ, 675, 784
Kains, N., Wyatt, M. C., & Greaves, J. S. 2011, MNRAS, 414, 2486
Kelsall, T., Weiland, J. L., Franz, B. A., Reach, W. T., Arendt, R. G., Dwek, E., Freudenreich, H. T., Hauser, M. G., Moseley, S. H., Odegard, N. P., Silverberg, R. F., & Wright, E. L. 1998, ApJ, 508, 44
Kennedy, G. M. & Wyatt, M. C. 2013, MNRAS, 433, 2334
Kennedy, G. M., Wyatt, M. C., Bailey, V., Bryden, G., Danchi, W. C., Defrère, D., Haniff, C., Hinz, P. M., Lebreton, J., Mennesson, B., Millan-Gabet, R., Morales, F., Panić, O., Rieke, G. H., Roberge, A., Serabyn, E., Shannon, A., Skemer, A. J., Stapelfeldt, K. R., Su, K. Y. L., & Weinberger, A. J. 2015, ApJS, 216, 23
Kennedy, G. M., Wyatt, M. C., Sibthorpe, B., Phillips, N. M., Matthews, B. C., & Greaves, J. S. 2012a, MNRAS, 426, 2115
Kennedy, G. M. et al. 2012b, MNRAS, 421, 2264
Krijt, S. & Kama, M. 2014, A&A, 566, L2
Kuchner, M. J. & Stark, C. C. 2010, AJ, 140, 1007
Lay, O. P. 2004, Appl. Opt., 43, 6100
Lestrade, J.-F. et al. 2012, A&A, 548, A86
Liou, J.-C. & Zook, H. A. 1999, AJ, 118, 580
Liou, J.-C., Zook, H. A., & Dermott, S. F. 1996, Icarus, 124, 429
Lisse, C. M., Wyatt, M. C., Chen, C. H., Morlok, A., Watson, D. M., Manoj, P., Sheehan, P., Currie, T. M., Thebault, P., & Sitko, M. L. 2012, ApJ, 747, 93
Meng, H. Y. A., Rieke, G. H., Su, K. Y. L., Ivanov, V. D., Vanzi, L., & Rujopakarn, W. 2012, ApJ, 751, L17
Mennesson, B., Millan-Gabet, R., Serabyn, E., Colavita, M. M., Absil, O., Bryden, G., Wyatt, M., Danchi, W., Defrère, D., Doré, O., Hinz, P., Kuchner, M., Ragland, S., Scott, N., Stapelfeldt, K., Traub, W., & Woillez, J. 2014, ApJ, 797, 119
Millan-Gabet, R., Serabyn, E., Mennesson, B., Traub, W. A., Barry, R. K., Danchi, W. C., Kuchner, M., Stark, C. C., Ragland, S., Hrynevych, M., Woillez, J., Stapelfeldt, K., Bryden, G., Colavita, M. M., & Booth, A. J. 2011, ApJ, 734, 67
Nesvorný, D., Jenniskens, P., Levison, H. F., Bottke, W. F., Vokrouhlický, D., & Gounelle, M. 2010, ApJ, 713, 816
Pawellek, N., Krivov, A. V., Marshall, J. P., Montesinos, B., Ábrahám, P., Moór, A., Bryden, G., & Eiroa, C. 2014, ApJ, 792, 65
Phillips, N. M., Greaves, J. S., Dent, W. R. F., Matthews, B. C., Holland, W. S., Wyatt, M. C., & Sibthorpe, B. 2010, MNRAS, 403, 1089
Rauer, H. et al. 2014, Experimental Astronomy, 38, 249
Reidemeister, M., Krivov, A. V., Stark, C. C., Augereau, J.-C., Löhne, T., & Müller, S. 2011, A&A, 527, A57
Rieke, G. H. et al. 2005, ApJ, 620, 1010
Roberge, A. et al. 2012, PASP, 124, 799
Rodriguez, D. R. & Zuckerman, B. 2012, ApJ, 745, 147
Schüppler, C., Löhne, T., Krivov, A. V., Ertel, S., Marshall, J. P., & Eiroa, C. 2014, A&A, 567, A127
Serabyn, E., Mennesson, B., Colavita, M. M., Koresko, C., & Kuchner, M. J. 2012, ApJ, 748, 55
Sierchio, J. M., Rieke, G. H., Su, K. Y. L., & Gáspár, A. 2014, ApJ, 785, 33
Smith, R., Wyatt, M. C., & Haniff, C. A. 2009, A&A, 503, 265
Song, I., Zuckerman, B., Weinberger, A. J., & Becklin, E. E. 2005, Nature, 436, 363
Stark, C. C. & Kuchner, M. J. 2008, ApJ, 686, 637
Stark, C. C., Roberge, A., Mandell, A., & Robinson, T. D. 2014, ApJ, 795, 122
Su, K. Y. L., Rieke, G. H., Stansberry, J. A., Bryden, G., Stapelfeldt, K. R., Trilling, D. E., Muzerolle, J., Beichman, C. A., Moro-Martin, A., Hines, D. C., & Werner, M. W. 2006, ApJ, 653, 675
Thureau, N. D., Greaves, J. S., Matthews, B. C., Kennedy, G., Phillips, N., Booth, M., Duchêne, G., Horner, J., Rodriguez, D. R., Sibthorpe, B., & Wyatt, M. C. 2014, MNRAS, 445, 2558
Trilling, D. E., Bryden, G., Beichman, C. A., Rieke, G. H., Su, K. Y. L., Stansberry, J. A., Blaylock, M., Stapelfeldt, K. R., Beeman, J. W., & Haller, E. E. 2008, ApJ, 674, 1086
van Lieshout, R., Dominik, C., Kama, M., & Min, M. 2014, A&A, 571, A51
Vitense, C., Krivov, A. V., Kobayashi, H., & Löhne, T. 2012, A&A, 540, A30
Weinberger, A. J., Bryden, G., Kennedy, G. M., Roberge, A., Defrère, D., Hinz, P. M., Millan-Gabet, R., Rieke, G., Bailey, V. P., Danchi, W. C., Haniff, C., Mennesson, B., Serabyn, E., Skemer, A. J., Stapelfeldt, K. R., & Wyatt, M. C. 2015, ApJS, 216, 24
Whipple, F. L., Southworth, R. B., & Nilsson, C. S. 1967, SAO Special Report, 239
Wyatt, M. C. 2005, A&A, 433, 1007
—. 2008, ARA&A, 46, 339
Wyatt, M. C., Dermott, S. F., Telesco, C. M., Fisher, R. S., Grogan, K., Holmes, E. K., & Piña, R. K. 1999, ApJ, 527, 918
Wyatt, M. C., Greaves, J. S., Dent, W. R. F., & Coulson, I. M. 2005, ApJ, 620, 492
Wyatt, M. C., Smith, R., Greaves, J. S., Beichman, C. A., Bryden, G., & Lisse, C. M. 2007a, ApJ, 658, 569
Wyatt, M. C., Smith, R., Su, K. Y. L., Rieke, G. H., Greaves, J. S., Beichman, C. A., & Bryden, G. 2007b, ApJ, 663, 365